arXiv:1205.0362v2 [hep-ph] 9 May 2012

Analyzing the anomalous dipole moment type couplings of t' quark with FCNC interactions at e^-e^+ colliders

A. T. Tasci,* A. Senol,† and C. Verep

Department of Physics, Kastamonu University, 37100, Kastamonu, Turkey

Abstract

In this study we examine both anomalous magnetic and dipole moment type couplings of fourth generation t' quark via its single production with subsequent dominant Standard Model decay modes at International Linear Collider (ILC) and Compact Linear Collider (CLIC). The signal and background cross sections are analyzed for the t' mass range of 400-800 GeV. We make the analysis to delimitate these anomalous couplings as well as to find the attainable integrated luminosities for 3σ observation limit.

PACS numbers: 12.60.-i, 14.65.Jk, 13.66.Hk

---

*Electronic address: atasci@kastamonu.edu.tr

†Electronic address: asenol@kastamonu.edu.tr

I. INTRODUCTION

The fourth generation, which occurs by extending the third generation of Standard Model (SM), is one of the simplest possibilities for physics beyond the SM and it is not ruled out experimentally. This extra generation of fermions may play a milestone role in the discovery of well known open questions such as the electroweak symmetry breaking [1–4], hierarchies of fermion mass spectrum and mixing angle in quark/lepton sectors [5–9], CP violation and flavor structure of standard theory [10–16]. In a recent study [17], experimental and theoretical statements about fourth SM generation are discussed. The precise determination of fourth generation quark properties may present the existence of new physics. A heavy down-type quark (b') with mass less than 480 GeV [18] and a up-type quark (t') with mass less than 404 GeV [19] are excluded at 95 % confidence level from proton-proton collisions at $\sqrt{s}$= 7 TeV ATLAS detector at the CERN Large Hadron Collider.

Searching for new sources of CP violation beyond the SM is an attractive subject in particle physics since, it explains the asymmetry between matter and anti-matter. CP violating anomalous flavor changing neutral current (FCNC) $tcZ/tc\gamma$ couplings have been considered in the literature before at hadron [20] and e^-e^+ [21, 22] colliders. These FCNC interactions offer an ideal place to search for new physics. Due to the large mass values, fourth generation quarks have crucial advantage to new interactions originating at a higher scale as in top quark physics.

Serious contributions can be expected for the production of the fourth generation fermions, due to the anomalous magnetic moment type interactions. Phenomenological studies with these anomalous effects of the fourth generation quarks have been performed at hadron colliders [23–28], at ep colliders [29, 30] and at linear colliders [31]. In this study, we investigate the single production of fourth generation t' quark at proposed linear colliders via both anomalous magnetic and dipole moment type interactions. International Linear Collider (ILC) [32] and Compact Linear Collider (CLIC) [33], the most popular proposed linear colliders on TeV scale, would complete the LHC results by performing precision measurements to provide necessary information about some parameters of the fourth generation. The aim of this study is to delimitate the anomalous magnetic and dipole moment type couplings of fourth generation t' quark from a detailed analysis for signal and background including Monte Carlo simulation with the effects of initial state radiation (ISR) and beamstrahlung (BS) in the e^+e^- collisions. Thus, we implement the related interaction vertices into the tree level event generator CompHEP package [34].

II. SINGLE PRODUCTION AND DECAY OF t' QUARK

The interaction Lagrangian for the fourth generation t' quark within the SM is given by

$$\begin{aligned}
L_s &= -g_e Q_{t'} \overline{t}' \gamma^\mu t' A_\mu \\
&\quad -g_s \overline{t}' T^a \gamma^\mu t' G^a_\mu \\
&\quad -\frac{g_e}{2 s_W c_W} \overline{t}' \gamma^\mu (g_V - g_A \gamma^5) t' Z^0_\mu \\
&\quad -\frac{g_e}{2\sqrt{2} s_W} V_{t' q_i} \overline{t}' \gamma^\mu (1-\gamma^5) q_i W^\pm_\mu + h.c.
\end{aligned} \tag{1}$$

where A_μ, G_μ, Z^0_μ and $W^\pm_\mu$ are the vector fields for photon, gluon, Z^0-boson and $W^\pm$-boson, respectively. g_e is the electro-weak coupling constant and g_s is the strong coupling constant. T^a are the Gell-Mann matrices; $Q_{t'}$ is the electric charge of fourth family quark t'. g_V and g_A are the vector and axial-vector type couplings of the neutral weak current with t' quark, θ_W is the weak mixing angle, $s_W = \sin\theta_W$ and $c_W = \cos\theta_W$. $V_{t'q}$ denotes the elements of extended 4×4 CKM mixing matrix which are constrained by flavor physics.

The anomalous magnetic and dipole moment type interactions among the fourth family quark t', ordinary quarks q, and the neutral gauge bosons $V = \gamma, Z, g$ can be described by an effective Lagrangian which contains the anomalous magnetic and dipole moment type couplings are given by

$$\begin{aligned}
L'_a &= \sum_{q_i=u,c,t} Q_{q_i} \frac{g_e}{\Lambda} \overline{t}' \sigma_{\mu\nu} (\kappa^{q_i}_\gamma - i\tilde{\kappa}^{q_i}_\gamma \gamma_5) q_i F^{\mu\nu} \\
&\quad + \sum_{q_i=u,c,t} \frac{g_e}{2\Lambda s_W c_W} \overline{t}' \sigma_{\mu\nu} (\kappa^{q_i}_Z - i\tilde{\kappa}^{q_i}_Z \gamma_5) q_i Z^{\mu\nu} \\
&\quad + \sum_{q_i=u,c,t} \frac{g_s}{2\Lambda} \overline{t}' \sigma_{\mu\nu} (\kappa^{q_i}_g - i\tilde{\kappa}^{q_i}_g \gamma_5) T^a q_i G^{\mu\nu}_a + h.c.
\end{aligned} \tag{2}$$

where $F^{\mu\nu}$, $Z^{\mu\nu}$ and $G^{\mu\nu}$ are the field strength tensors of the gauge bosons; $\sigma_{\mu\nu} = i(\gamma_\mu\gamma_\nu - \gamma_\nu\gamma_\mu)/2$; Q_{q_i} is the electric charge of the quark (q). $\kappa_\gamma(\tilde{\kappa}_\gamma)$, $\kappa_Z(\tilde{\kappa}_Z)$ and $\kappa_g(\tilde{\kappa}_g)$ are the anomalous magnetic (dipole) moment type couplings with photon, Z boson and gluon, respectively. Note that $\tilde{\kappa}$' s are CP violating. Λ is the cut off scale of new interactions.

Branching ratios (BR) for SM decay channels $(Wd(s,b))$ and anomalous decay channels $(Vu(c,t))$ of t' quark which are calculated by using Lagrangians (1) and (2), respectively;

and total decay widths of t' quark are given in Table I by taking all anomalous magnetic and dipole moment type couplings over Λ is equal to 0.1 TeV^{-1}. When calculating SM BR's, we use the approximate values of the 4×4 CKM matrix elements given in Ref. [35], which are motivated by the constraints from the Kaon decay and $Z \to b\bar{b}$ decay. As seen from this table SM t' decay channel $t' \to Wb$ is dominant approximately with 64% BR.

TABLE I: Total decay widths (GeV) and branching ratios (%) of the t' quark in both chiral and anomalous interactions.

$m_{t'}$	Wd	Wb	Ws	Zu(c)	Zt	gu(c)	gt	γu(c)	γt	Γ_{tot}(GeV)
300	0.026	66	18	0.40	0.08	6.5	1.9	0.15	0.042	0.65
400	0.026	65	17	0.41	0.20	6.4	3.4	0.14	0.075	1.57
500	0.026	64	17	0.42	0.28	6.3	4.3	0.14	0.095	3.10
600	0.026	64	17	0.42	0.32	6.3	4.8	0.14	0.110	5.40
700	0.025	64	17	0.43	0.35	6.2	5.1	0.14	0.110	8.61
800	0.025	64	17	0.43	0.37	6.2	5.4	0.14	0.120	12.90

The contributing tree level Feynman Diagrams for the anomalous single production of t' quark in e^+e^- collision are shown in Fig. 1.

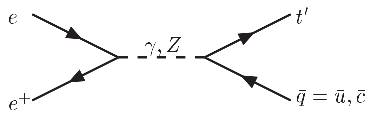

FIG. 1: Feynman diagram for single production of t' in e^+e^- collision.

In Fig. 2, the total cross sections for single production of t' quark are plotted at collision center of mass energies (a) 0.5 TeV and (b) 3 TeV with respect to their masses. Here, we assume κ_γ=κ_Z=κ_g=κ and $\tilde{\kappa}_\gamma$=$\tilde{\kappa}_Z$=$\tilde{\kappa}_g$=$\tilde{\kappa}$ by taking $\kappa/\Lambda = \tilde{\kappa}/\Lambda = 0.1$ TeV^{-1}, unless stated otherwise, we have used these values in our calculations. Initial state radiation (ISR) and beamstrahlung (BS) is a specific feature of the linear colliders. We take the beam parameters that are given for the ILC and CLIC in Table II, when calculating the ISR and BS effects. As it is seen from Fig. 2, the effects of ISR and BS can lead to a decrease in the cross section. Here, the dotted line denotes the cross section including ISR+BS effects while solid

TABLE II: Main parameters of ILC and CLIC. Here, N is the number of particles in bunch. σ_x and σ_y are beam sizes, σ_z is the bunch length.

Parameters	ILC	CLIC
$E_{cm}(\sqrt{s})$ TeV	0.5	3
$L(10^{34}cm^{-2}s^{-1})$	2	5.9
$N(10^{10})$	2	0.372
σ_x (nm)	639	45
σ_y (nm)	5.7	1
σ_z (μm)	300	44

line denotes without ISR+BS effects. Hereafter, we take into account ISR+BS effects in all our numerical calculations.

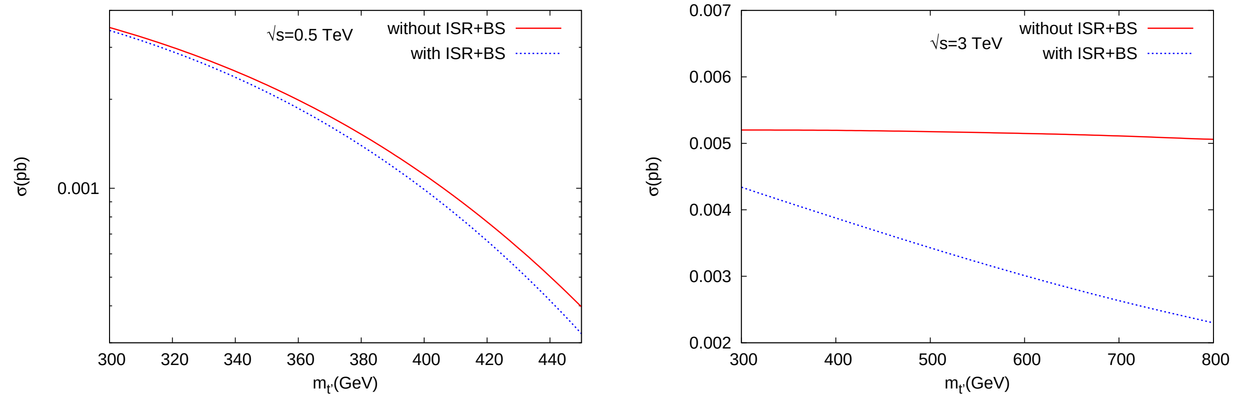

(a)

(b)

FIG. 2: The total cross sections at (a) $\sqrt{s}$ =0.5 TeV and (b) $\sqrt{s}$ =3 TeV for the process $e^+e^- \to t'\bar{q}$ ($\bar{q} = \bar{u}, \bar{c}$), as function of t' mass.

III. SIGNAL AND BACKGROUND ANALYSIS

The single production of fourth generation t' quark of signal process including dominance of the SM decay mode over anomalous decay is $e^+e^- \to t'\bar{q}_i \to W^+b\ \bar{q}_i$ where, $\bar{q}_i = \bar{u}, \bar{c}$. The dominant source of SM background process is $e^+e^- \to W^+b\ \bar{q}_i$ for the corresponding signal processes. In Fig. 3, the transverse momentum (p_T) distributions of the final state b

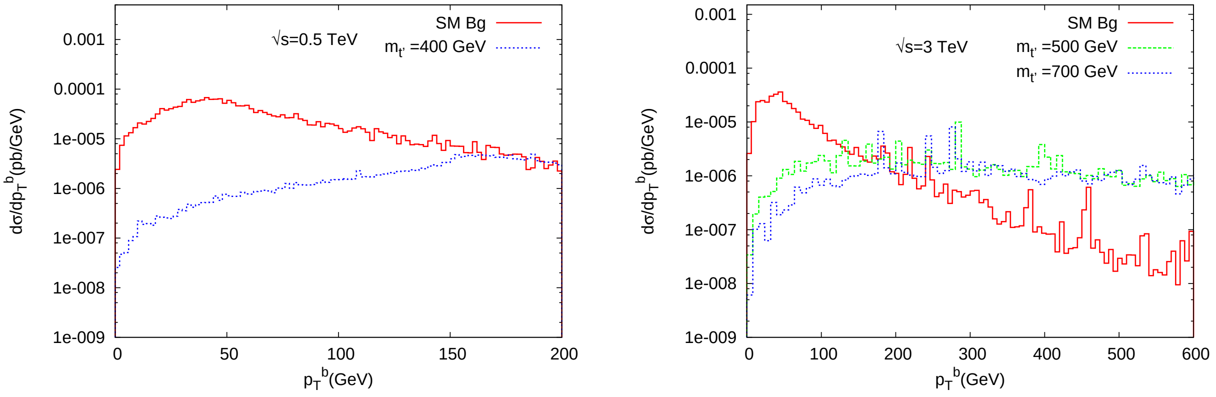

(a) (b)

FIG. 3: The differential cross section depending on the transverse momentum of the final state b quark of process $e^+e^- \to W^+b\ \bar{q}(\bar{q} = \bar{u}, \bar{c})$ for SM background (solid line) and signal with different mass values of t' quarks at (a) $\sqrt{s}$ =0.5 TeV and (b) $\sqrt{s}$ =3 TeV.

quark for signal and background are shown for ILC and CLIC options. We applied a p_T cut of $p_T > 50$ GeV to reduce the background, comparing the signal p_T distribution of b quark with that of the corresponding background.

In Fig. 4, we plot the rapidity distributions of final state b quark in signal and background processes. According to these figures, the cut $|\eta^b| < 2.5$ can be applied to suppress the background while the signal remains almost unchanged. In Fig. 5, the invariant mass

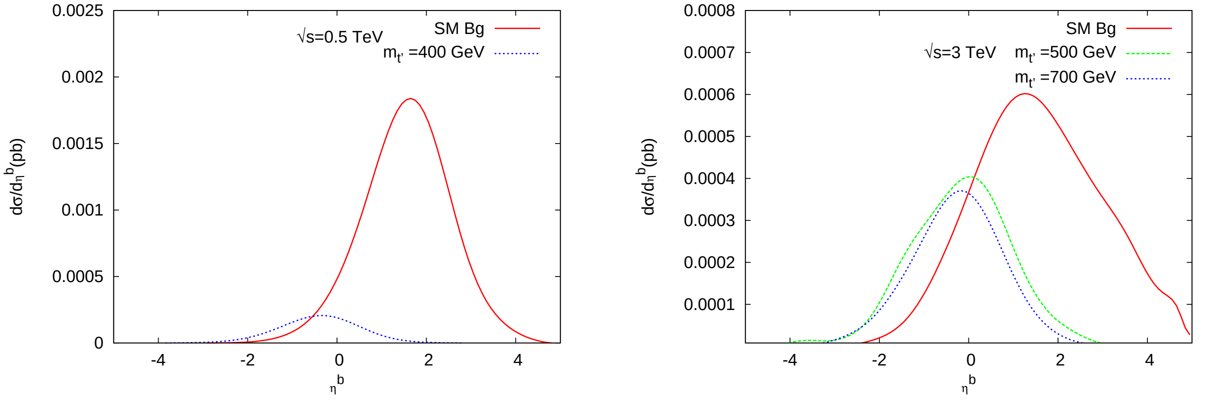

(a) (b)

FIG. 4: The rapidity distribution of the final state b quark at (a) $\sqrt{s}$ =0.5 TeV and (b) $\sqrt{s}$ =3 TeV for the process $e^+e^- \to W^+b\bar{q}$ ($\bar{q} = \bar{u}, \bar{c}$).

distributions for the W^+b system in the final state are plotted. From these figures, we can see that the signal has a peak around mass of t' quark over the background.

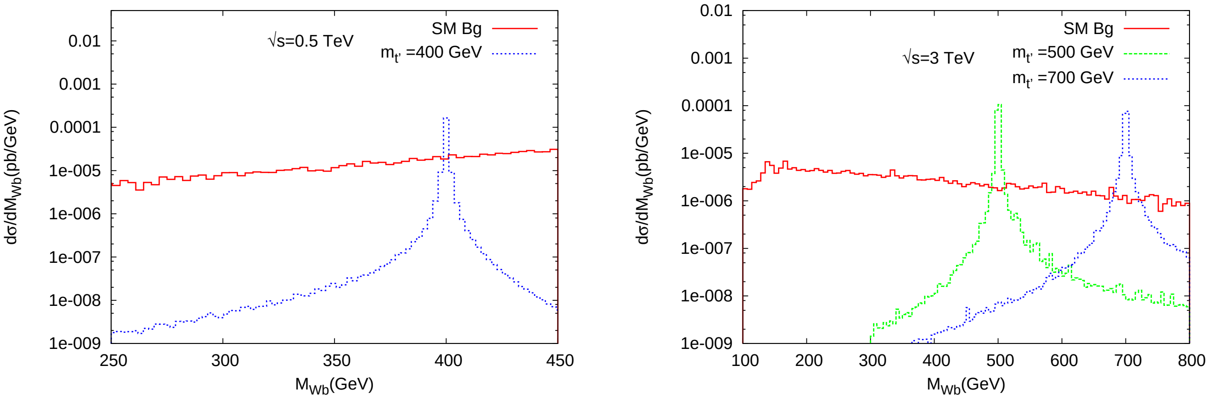

(a) (b)

FIG. 5: The invariant mass distribution of the final state Wb system for SM background (solid line) and signal from t' decay for (a) $m_{t'} = 300$ GeV (dotted line) at $\sqrt{s}$ =0.5 TeV and (b) $m_{t'} = 300$ GeV (dotted line), $m_{t'} = 500$ GeV (dashed line) and $m_{t'} = 700$ GeV (dot-dashed line) at $\sqrt{s}$ =3 TeV.

In Tables III and IV, we calculate the signal and background cross sections and the statistical significance (SS) in order to discuss the observability of the fourth generation t' quark at linear colliders for ILC and CLIC parameters, respectively. We obtain the SS of the signal by using the formula [36],

$$SS = \sqrt{2L_{int}\epsilon[(\sigma_S + \sigma_B)\ln(1 + \sigma_S/\sigma_B) - \sigma_S]}.$$

where σ_S is the the signal and σ_B is the background cross sections, respectively. We take into account finite energy resolution of the detectors for realistic analysis. In our numerical calculations we use the mass bin width $\Delta m = max(2\Gamma, \delta m)$ to count signal and background events with the mass resolution δm. We also apply the mentioned p_T and η cuts assuming the integrated luminosities given in Table II. In the signal and background processes, we consider the final state W boson decays leptonicaly via $W^{\pm} \to l^{\pm}\nu_l$ where $l^{\pm} = e^{\pm}, \mu^{\pm}$ and we assume the b-tagging efficiency as $\epsilon = 50\%$. From Tables III and IV, with the observability criteria of 3σ, we see the t' quark can be observed in the scanned mass interval of 400-800 GeV at the CLIC while up to about 400 GeV at the ILC.

TABLE III: The signal and background cross sections and signal Statistical Significance (SS) for the ILC at $\sqrt{s} = 0.5$ TeV with integrated luminosity of $2{\times}10^5$ pb^{-1}.

$m_{t'}$(GeV)	σ_S(pb)	σ_B(pb)	SS
400	3.32×10^{-4}	2.81×10^{-5}	8.72
450	8.93×10^{-5}	7.21×10^{-5}	2.30

TABLE IV: The signal and background cross sections and signal Statistical Significance (SS) for the CLIC at $\sqrt{s} = 3$ TeV with integrated luminosity of $5.9{\times}10^5$ pb^{-1}.

$m_{t'}$(GeV)	σ_S(pb)	σ_B(pb)	SS
400	1.06×10^{-3}	3.66×10^{-6}	25.34
500	9.49×10^{-4}	5.95×10^{-6}	22.50
600	8.41×10^{-4}	8.92×10^{-6}	19.84
700	7.46×10^{-4}	1.14×10^{-5}	17.77
800	6.59×10^{-4}	1.37×10^{-5}	15.95

So far, we assume the anomalous couplings are equal to each other. After this point, we will focus on limiting the anomalous magnetic and dipole moment type couplings. Firstly, in Fig. 6, we present the 3σ contour plot for $\tilde{\kappa}/\Lambda$ - κ/Λ plane at a) $\sqrt{s} = 0.5$ TeV with $m_{t'}$=400 GeV and b) $\sqrt{s} = 3$ TeV with $m_{t'}$=500 GeV. According to these figures, the lower limits of κ/Λ and $\tilde{\kappa}/\Lambda$ are about 0.06 TeV^{-1} at the ILC and 0.03 TeV^{-1} at the CLIC energies.

To analyze the case of $\tilde{\kappa}_\gamma/\Lambda \neq \tilde{\kappa}_Z/\Lambda$, the 3σ contour plots for the anomalous couplings in the $\tilde{\kappa}_Z/\Lambda - \tilde{\kappa}_\gamma/\Lambda$ plane are presented in Fig. 7 at a) $\sqrt{s} = 0.5$ TeV with $m_{t'}$=400 GeV and b) $\sqrt{s} = 3$ TeV with $m_{t'}$=500 GeV by taking into account different values of κ/Λ. According to these figures the lower limits of $\tilde{\kappa}_\gamma/\Lambda$ and $\tilde{\kappa}_Z/\Lambda$ are about 0.09 TeV^{-1} at the ILC and 0.04 TeV^{-1} at the CLIC energies with κ/Λ=0.01 TeV^{-1}. In Figs. 6 and 7, area of the allowed parameter space of t' quark is above the lines by taking into account the extended CKM matrix elements.

We plot the lowest necessary luminosities with 3σ observation limits at (a) $\sqrt{s} = 0.5$ TeV and (b) 3 TeV energies depending on anomalous couplings in Fig. 8. In the case of κ/Λ=$\tilde{\kappa}/\Lambda$=0.1 TeV^{-1}, it is seen that from these figures, the fourth generation t' quarks with masses 400 and 500 GeV can be observed at 3σ observation limit with lowest integrated

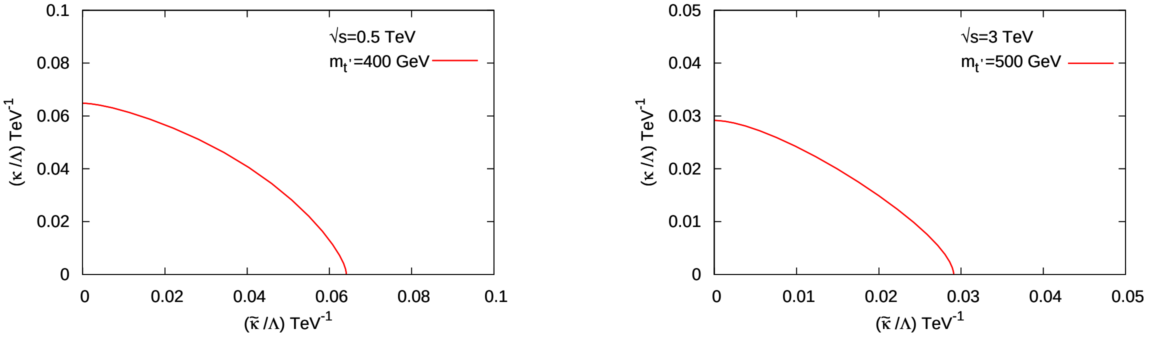

(a)

(b)

FIG. 6: The 3σ contour plot for the anomalous couplings reachable at (a) $\sqrt{s}$ =0.5 TeV with L_{int}=2×10^5 pb^{-1} and (b) $\sqrt{s}$ =3 TeV with L_{int}=5.9×10^5 pb^{-1}.

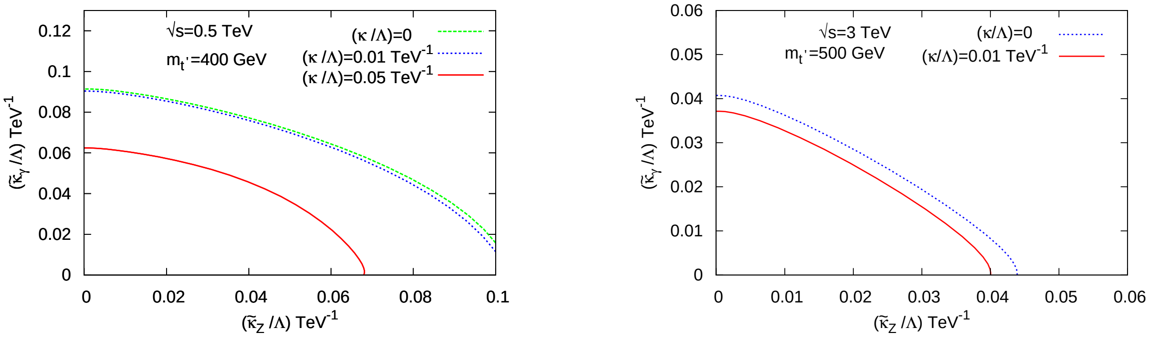

(a)

(b)

FIG. 7: The 3σ contour plot for the anomalous dipole moment type couplings reachable at (a) $\sqrt{s}$ =0.5 TeV with $m_{t'}$=400 GeV and (b) $\sqrt{s}$ =3 TeV with $m_{t'}$=500 GeV.

luminosity about 2×10^5 pb^{-1} at ILC and 3×10^4 pb^{-1} at CLIC, respectively.

IV. CONCLUSION

The anomalous FCNC interactions of the fourth generation quarks could be important for some parameter regions due to the expected large masses. The sensitivity to the anomalous couplings (κ, $\tilde{\kappa}$) and ($\tilde{\kappa}_\gamma$, $\tilde{\kappa_Z}$) can be obtained at ILC about (0.06, 0.06) and (0.06, 0.07) for κ=0.05 with $m_{t'}$=400 GeV, at CLIC these values can be obtained about (0.03, 0.03)

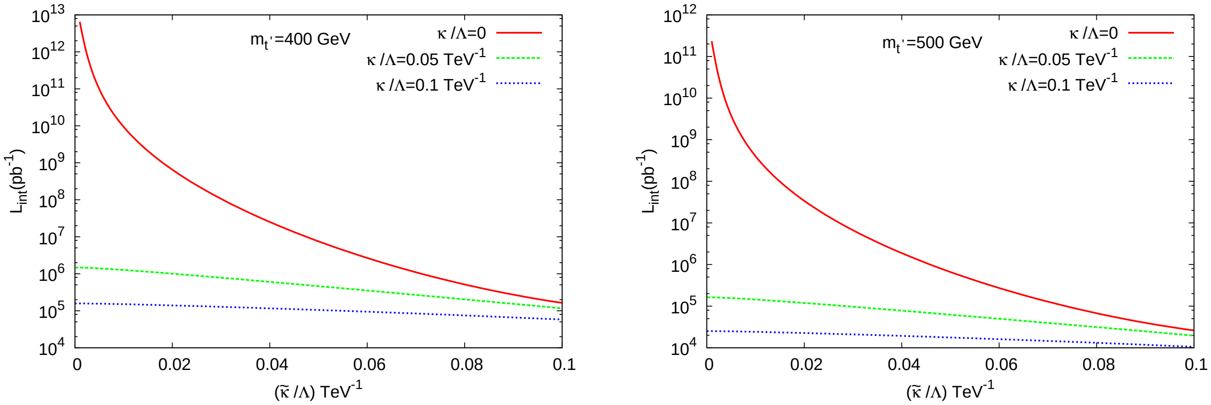

(a)

(b)

FIG. 8: The attainable integrated luminosity for 3σ observation limit at (a) $\sqrt{s}$ =0.5 TeV (b) $\sqrt{s}$ =3 TeV depending on anomalous dipole moment type couplings.

and (0.038, 0.04) for κ=0.01 with $m_{t'}$=500 GeV for Λ= 1 TeV by taking into account the parametrization for extended CKM matrix elements. We also find the lowest necessary luminosity limit values as 2×10^5 pb^{-1} at ILC and 3×10^4 pb^{-1} at CLIC.

Acknowledgments

This research has been supported by Kastamonu University Scientific Research Projects Coordination Department.

[1] B. Holdom, Phys. Rev. Lett. **57**, 2496 (1986) [Erratum-ibid. **58**, 177 (1987)].

[2] C. T. Hill, M. A. Luty and E. A. Paschos, Phys. Rev. D **43**, 3011 (1991).

[3] T. Elliott and S. F. King, Phys. Lett. B **283**, 371 (1992).

[4] P. Q. Hung and C. Xiong, Nucl. Phys. B **848**, 288 (2011).

[5] B. Holdom, JHEP **0608**, 076 (2006).

[6] P. Q. Hung and M. Sher, Phys. Rev. D **77**, 037302 (2008).

[7] P. Q. Hung, C. Xiong, Phys. Lett. **B694**, 430-434 (2011).

[8] P. Q. Hung and C. Xiong, Nucl. Phys. B **847**, 160 (2011).

[9] O. Cakir, A. Senol and A. T. Tasci, Europhys. Lett. **88**, 11002 (2009).

[10] W. S. Hou and C. Y. Ma, Phys. Rev. D **82**, 036002 (2010).

[11] S. Bar-Shalom, D. Oaknin and A. Soni, Phys. Rev. D **80**, 015011 (2009).

[12] A. J. Buras, B. Duling, T. Feldmann, T. Heidsieck, C. Promberger and S. Recksiegel, JHEP **1009**, 106 (2010).

[13] A. Soni, A. K. Alok, A. Giri, R. Mohanta and S. Nandi, Phys. Lett. B **683**, 302 (2010).

[14] O. Eberhardt, A. Lenz and J. Rohrwild, Phys. Rev. D **82**, 095006 (2010).

[15] A. Soni, A. K. Alok, A. Giri, R. Mohanta and S. Nandi, Phys. Rev. D **82**, 033009 (2010).

[16] A. K. Alok, A. Dighe and D. London, Phys. Rev. D **83**, 073008 (2011).

[17] B. Holdom, W. S. Hou, T. Hurth, M. L. Mangano, S. Sultansoy and G. Unel, PMC Phys. A **3**, 4 (2009).

[18] G. Aad *et al.* [ATLAS Collaboration], arXiv:1202.6540 [hep-ex].

[19] G. Aad *et al.* [ATLAS Collaboration], arXiv:1202.3076 [hep-ex].

[20] T. Han, K. Whisnant, B. L. Young and X. Zhang, Phys. Rev. D **55**, 7241 (1997).

[21] T. Han and J. L. Hewett, Phys. Rev. D **60**, 074015 (1999).

[22] A. T. Alan, A. Senol and A. T. Tasci, J. Phys. G **29**, 279 (2003).

[23] E. Arik, O. Cakir, S. Sultansoy, Europhys. Lett. **62**, 332-335 (2003).

[24] E. Arik, O. Cakir, S. Sultansoy, Phys. Rev. **D67**, 035002 (2003).

[25] I. T. Cakir, H. Duran Yildiz, O. Cakir *et al.*, Phys. Rev. **D80**, 095009 (2009).

[26] R. Ciftci, Phys. Rev. **D78**, 075018 (2008).

[27] M. Sahin, S. Sultansoy, S. Turkoz, Phys. Rev. **D82**, 051503 (2010).

[28] O. Cakir, I. T. Cakir, A. Senol and A. T. Tasci, J. Phys. G **39**, 055005 (2012).

[29] A. T. Alan, A. Senol, O. Cakir, Europhys. Lett. **66**, 657-660 (2004).

[30] R. Ciftci and A. K. Ciftci, arXiv:0904.4489 [hep-ph].

[31] A. Senol, A. T. Tasci and F. Ustabas, Nucl. Phys. B **851**, 289 (2011).

[32] J. Brau, (Ed.) *et al.* [ILC Collaboration], "ILC Reference Design Report: ILC Global Design Effort and World Wide Study," arXiv:0712.1950 [physics.acc-ph].

[33] L. Linssen, A. Miyamoto, M. Stanitzki and H. Weerts, "Physics and Detectors at CLIC: CLIC Conceptual Design Report," arXiv:1202.5940 [physics.ins-det].

[34] A. Pukhov *et al.*, arXiv:hep-ph/9908288.

[35] W. S. Hou and C. Y. Ma, Phys. Rev. D **82**, 036002 (2010).

[36] G. L. Bayatian *et al.* [CMS Collaboration], J. Phys. G **34**, 995 (2007).